

PAPER • OPEN ACCESS

Operation features of the pulse penning ion source in the transition pressure range

To cite this article: N V Mamedov *et al* 2019 *J. Phys.: Conf. Ser.* **1393** 012047

View the [article online](#) for updates and enhancements.



IOP | ebooks™

Bringing you innovative digital publishing with leading voices to create your essential collection of books in STEM research.

Start exploring the collection - download the first chapter of every title for free.

Operation features of the pulse penning ion source in the transition pressure range

N V Mamedov^{1,2}, S P Maslennilov^{1,2}, A A Solodovnikov¹ and D I Yurkov^{1,2}

¹ Dukhov Automatics Research Institute (VNIIA), Federal State Unitary Enterprise, 22 Sushevskaya Str., Moscow, 127055, Russia

² National Research Nuclear University MEPhI, 31 Kashirskoye Sh., Moscow, 115409, Russia

E-mail: vnii4@vniia.ru

Abstract. The paper presents the results of experiments studying the dependence of discharge and extracted currents on the pressure of pulsed penning ion source (PIS). A comparative analysis of the amplitude-time and current-voltage characteristics of PIS for the various anode voltage amplitudes, pulse repetition rates, pulse durations, magnitudes (and configurations) of the magnetic field is presented. The obtained results reveal the existence of different (stable and unstable) discharge modes depending on the operating conditions of the power supply system and the pressure range of the working gas (deuterium). The features of current waveforms in the transitional pressure range 0.5–2 mTorr are defined.

1. Introduction

The ExB gas discharge is widely used in various fields of science and technology [1]. In particular the penning discharge is effectively used in ion sources (IS) for the miniature linear accelerators [2].

There are several modes of the penning discharge combustion depending on the physical parameters (anode voltage, magnetic field magnitude, working gas pressure) [3–7]. The discharge mode significantly affects the potential and the electron density distributions inside the discharge cell as well as the rate of the discharge development and, as the consequence, the ion beam density and the efficiency of the ion extraction. In the literature [3, 7] the generally accepted classification of the discharge modes is based on the pressure (for given pressure value it depends on the magnetic field magnitude, the anode voltage and the geometric parameters of the discharge cell):

1. High voltage discharge mode at low pressure. The characteristic pressure $p \leq 10^{-4}$ torr.

This mode is divided into three parts depending on the magnitude of the magnetic field. For the discharge current density less than $10 \mu\text{A}\cdot\text{cm}^{-2}$, there is virtually no distortion of the potential distribution within the discharge cell. This mode is called Townsend mode, and is usually realized at the discharge ignition or at very low magnetic fields.

With the magnetic field increase, electrons start moving along the closed cycloids and move to the anode only as a result of collisions with the gas atoms. Ions move freely (almost without collisions) to the cathode along the electric field lines, without experiencing serious influence of the magnetic field. As a result, cloud of negative charge is formed between the cathodes. Depending on the magnetic field magnitude, modes of low magnetic field (LMF) and high magnetic field (HMF) are distinguished. In



the LMF mode, the discharge current depends linearly on the magnetic field. The negative space charge distribution in the anode cylinder is almost uniform. There is a near-cathode and near-anode area of potential drop. As the magnetic field increases, the negative spatial charge builds up, eventually leading to the potential drop on the axis up to the cathode level (equal to zero). The potential drop is now localized at the anode and the discharge shifts into HMF mode. Plasma region free from the electric field forms around the axis, surrounded by an electron cloud adjacent to the anode. At the same time, the rate of ions leaving the cathodes becomes comparable to the rate of electrons leaving the anode [8]. In the HMF mode, the discharge current depends on the magnetic field weakly [7] (or in some cases decreases with the growth of B_z [3]). The characteristic density of the discharge current is usually of several $\text{mA}\cdot\text{cm}^{-2}$.

2. *Transitional discharge mode.* Characteristic pressure range $\sim 10^{-4}$ Torr– 10^{-3} Torr.

It is divided into two components – transitional mode (TM) and high-pressure mode (HP). At the elevated pressures, despite the life-time of the electron in the discharge volume decreases the total number of the electron collisions (both ionizing and not) remains virtually unchanged. The density of electrons does not change, whereas the concentration of ions increases – the quasi-neutral plasma is formed in the discharge. The electron shell (with nonuniform azimuthally distribution of the charge) still persists near anode in Transition mode (TM), but there is already cathode potential drop which is typical for a glow discharge. The discharge voltage is still high (several keV), and the current can reach several tens of milliamps (depending on type of gas). It is noted that this transition mode has strong instability, which is not fully studied yet [4].

However, in the course of transition to the HP-mode (with an even greater pressure increase), the anode drop suddenly disappears; the density of the discharge current increases exponentially from $\sim \text{mA}\cdot\text{cm}^{-2}$ to $\sim \text{A}\cdot\text{cm}^{-2}$, the potential distribution becomes similar to the distribution in the normal glow discharge. The difference is in the presence of a strong axial electric field in the central plasma region.

3. *Glow reflective discharge*

At higher pressures (in [7] at $P \gg 10^{-3}$ Torr), the magnetic field no longer plays a determining role in discharge maintaining. The free path of the electron becomes less than the cell length. A glow discharge (GD) with an unusual configuration of the electrodes forms. At discharge currents with a density of $\sim \text{A}\cdot\text{cm}^{-2}$ and in the absence of cathode spots, the discharge is similar to an abnormal glow discharge with a positive column in a magnetic field. With the increase in current and the formation of a cathode spot, the smoldering reflective discharge can switch into an arc (arc reflective discharge).

Unfortunately, in the presented reviews [3–7] and modern papers [9–17] not enough information about the behavior of the extraction ion current for the combustion mode discharge (at a variation of pressure, stress and magnetic field) is given. The stable operation of PIS requires linear dependence of the discharge current and the extracted ion current on the pressure, so it is essential to determine the exact boundary of the transition pressure. Also, for impulse PIS, a significant criterion is the rectangular shape of the extracted current pulse with short front and edge fronts, which does not change its shape in a given pressure range [16].

2. Experimental result

The diagnostic setup for the study of the PIS discharge modes is created in Dukhov Research Institute of Automatics (VNIIA). The investigated PIS (described in [17]) is connected to the vacuum system of the setup (see figure 1) using standard pumping rods.

The pressure in PIS is controlled by the Pfeiffer PKR 251. In order to determine the relationship between the true pressure directly in the PIS volume and the vacuum gauge data, appropriate estimates and experimental calibrations are carried out using an additional measuring volume (metal-glass cylinder with its own built-in getter) and vacuum gauge Varian FRG-702. The maximum residual

pressure is 10^{-6} Torr, the operating pressure varied from 0.1 to 10 mTorr (gas – deuterium). The relative error of the pressure measurements is no more than 45 %.

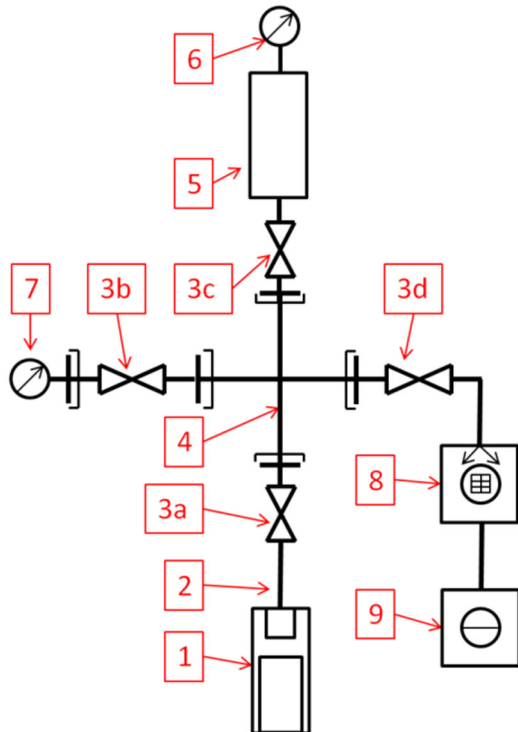


Figure 1. Scheme of the experimental setup: 1 – investigated pulse penning ion source (PIS), 2 – standard pumping rods, 3a, 3b, 3c, 3d – valves Swagelok SS-4H, 4 – cross tube fitting Swagelok SS-400-4, 5 – measuring volume (metal-glass container) – for pressure calibration in PIS, 6 – compact vacuum gauge Varian FRG-702, 7 – compact vacuum gauge Pfeiffer PKR 251, 8 – turbomolecular pump Pfeiffer TC600, 9 – oil-free membrane pump Vacuubrand MZ-2D. Working gas is deuterium, D₂.

The developed system of power supply provides opportunities for research of PIS in the direct or pulse current modes, and also allows real-time measurement of cathode, anode and extracted currents (see figure 2). The experimental setup measurement system is fully automated, to create a control loop with pressure feedback, a virtual proportional-integral-differentiating (PID) regulator is implemented in the control program. To create an axially symmetric magnetic field (of different size and configuration), a current solenoid was used in PIS.

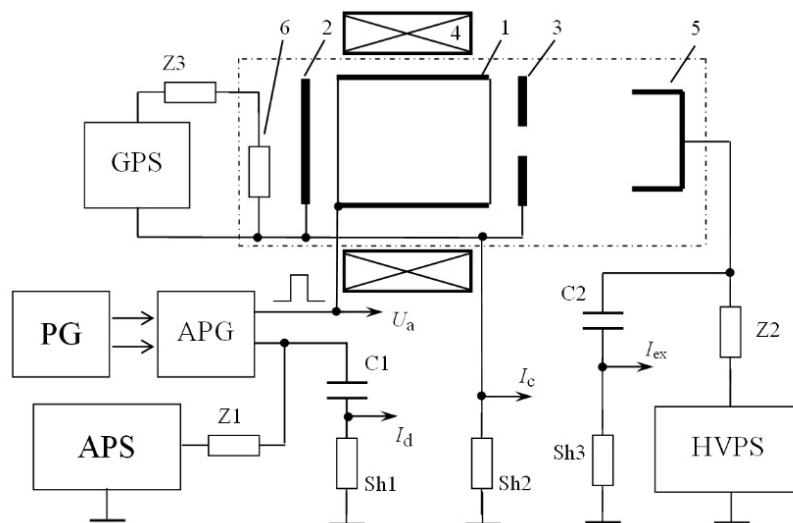


Figure 2. The experimental setup power supply system for studies of discharge modes in PIS with grounding pins built-in getter: 1 – anode, 2 – cathode, 3 – cathode, 4 – solenoid, 5 – target; 6 – heater getter (gas storage). GPS – getter power supply; HVPS high-voltage power supply; APS – Anode power supply; APG – Anode pulse generator; PG – pulse generator

The dependences of the discharge current (I_d) and the extraction current (I_{ex}) on the pressure are presented on figure 3. PIS operated in stationary ($U_a = 2$ kV) and pulse-periodic power mode ($U_a = 2$ kV, $f = 10$ kHz, $t_{pulse} = 30$ μ s and $U_a = 2$ kV, $f = 2$ kHz, $t_{pulse} = 150$ μ s). The discharge current released

on the plateau (in the pulsed mode of supply) is equivalent to the current in the continuous mode of supply at the same gas pressure. In the stationary power mode, the discharge ignition pressure is $P \sim 3 \times 10^{-5}$ Torr ($I_d \sim 10\text{--}30 \mu\text{A}$). At P from $\sim 3 \times 10^{-5}$ to 8×10^{-4} Torr discharge current increases linearly with increasing pressure. For long pulses ($t_{pulse} = 150 \mu\text{s}$), the discharge ignition takes place in the range of 0.2–0.4 mTorr, for short pulses ($t_{pulse} = 30 \mu\text{s}$) the ignition happens at $P \sim 0.8\text{--}1$ mTorr.

Discharge current instabilities are observed at pressure lower than 2 mTorr. The current pulses have a triangular pulse spikes (see figure 4). At pressures $P \sim 0.8\text{--}2$ mTorr discharge current decrease I_d from $\sim 300 \mu\text{A}$ to $\sim 200 \mu\text{A}$. It can be argued that the regime of the discharge shifts to transition mode (TM).

At pressures from 3 to 6 mTorr, the discharge is stable, the oscillograph chart have a "constant" rectangular shape, while the discharge current amplitude increases from 200 to $500 \mu\text{A}$ with an increase in pressure (similarly the extraction current amplitude increases from 180 to $230 \mu\text{A}$). A further pressure increase (from 7 mTorr) leads to a sharp increase in the discharge current (to values above 1 mA). The discharge becomes a high-pressure mode (HP) characterized by the exponential growth of the discharge current with pressure.

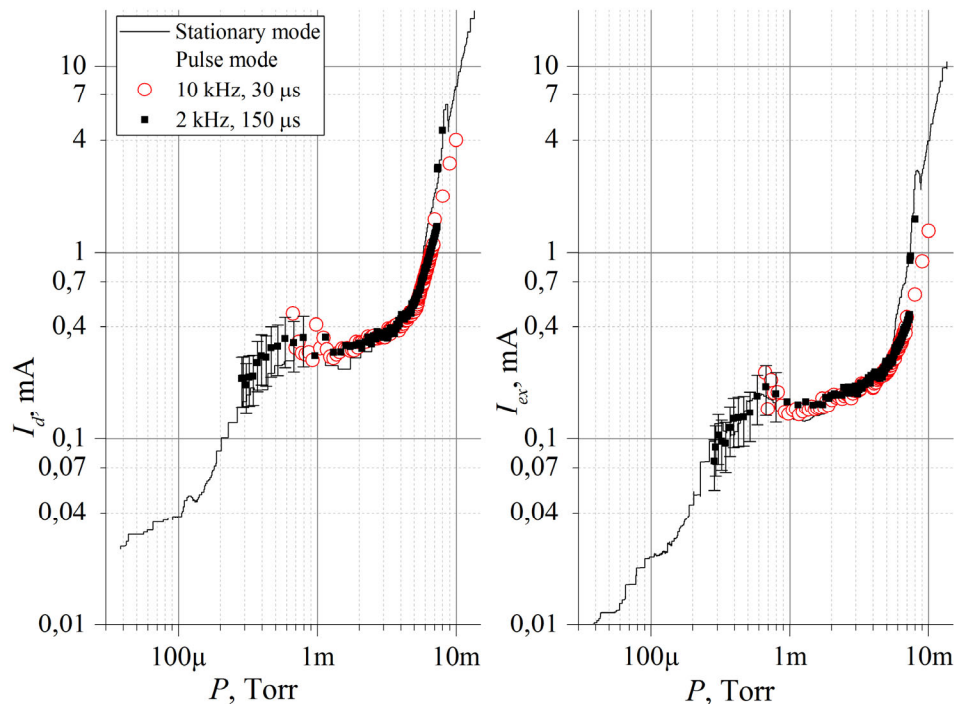


Figure 3. Dependences of discharge current (I_d) and extraction current (I_{ex}) on the pressure during operation of PIS in stationary (continuous line) and pulse-periodic (point) power supply mode. $f = 10$ kHz, $t_{pulse} = 30 \mu\text{s}$ – circles. $f = 2$ kHz, $t_{pulse} = 150 \mu\text{s}$ – squares.

At constant anode voltages in the range of 2.4–3.0 kV, the curve of the discharge current (and the extraction current) dependence on the pressure is shifted towards lower pressure values, while the discharge current is in the range of 200–800 μA at pressures below 1 mTorr (see figure 5). On contrary, in pulsed-periodic mode ($t_{pulse} = 30 \mu\text{s}$), the increase of the anode voltage did not result in a significant shift of the $I_d(P)$ and $I_{ex}(P)$ curves to the lower pressure range. The increase in anode voltage leads to a slight improvement of amplitude-time characteristics. For example, at a pressure of 3 mTorr, with increase in voltage, the delay time (time between current flash and the voltage pulse) (t_{delay}) decreases from 10 to 8 μs , and the front time of the current pulse (t_{front}) decreases from 2.0 to 1.5 μs (see figure 6). At a pressure of 6 mTorr, the delay time decreases from 6 to 5 μs , and the leading edge time from 1.2 to 1.0 μs .

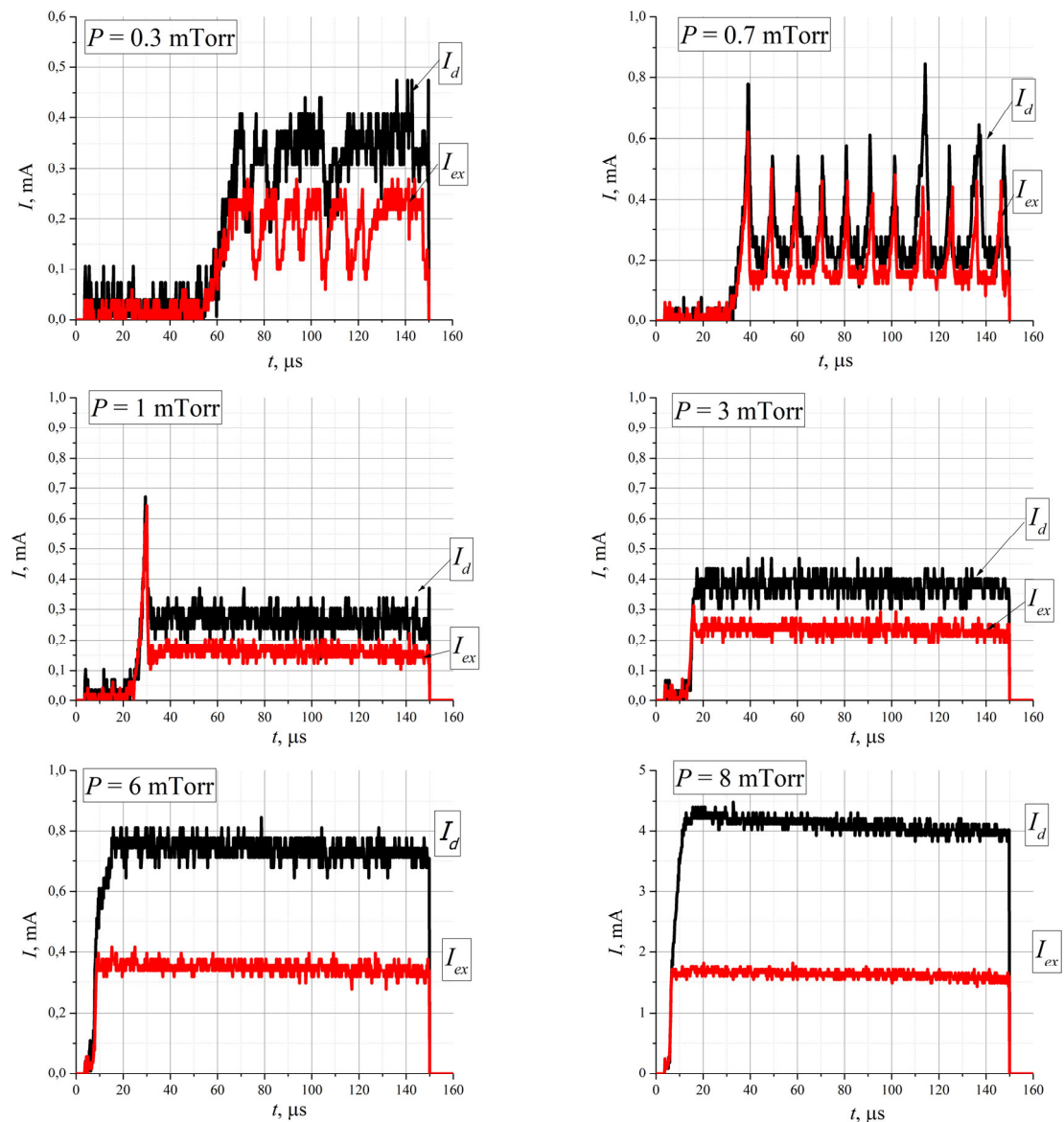


Figure 4. Examples of current pulse waveforms in the transient pressure range (I_d – discharge current, I_{ex} – extraction current). $U_a = 2$ kV, $f = 2$ kHz, $t_{pulse} = 150$ μ s.

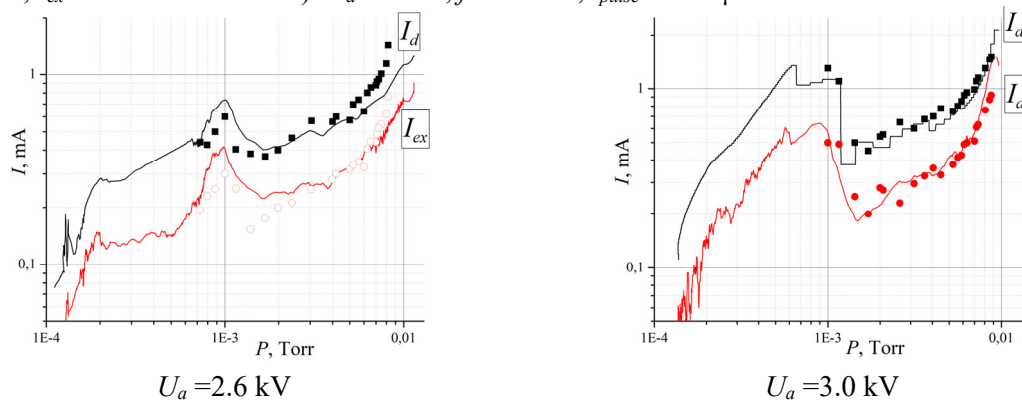


Figure 5. Dependence of discharge current I_d (black) and extraction current I_{ex} (red) on pressure at different anode voltages. Continuous lines – constant power mode, points – pulse power mode (10 kHz, 30 μ s).

With anode voltage increase (in pulsed power supply), the discharge ignition range remains the same $p \sim 0.8\text{--}1\text{mTorr}$. Moreover, in the region of $\sim 1\text{ mTorr}$, the shape of the flash is unstable and has either a triangular emission or fluctuations in the maximum. At high pressures ($P > 4\text{ mTorr}$) or at voltages above 2.2 kV, a peak appears in the waveform at the leading edge of the spectrum.

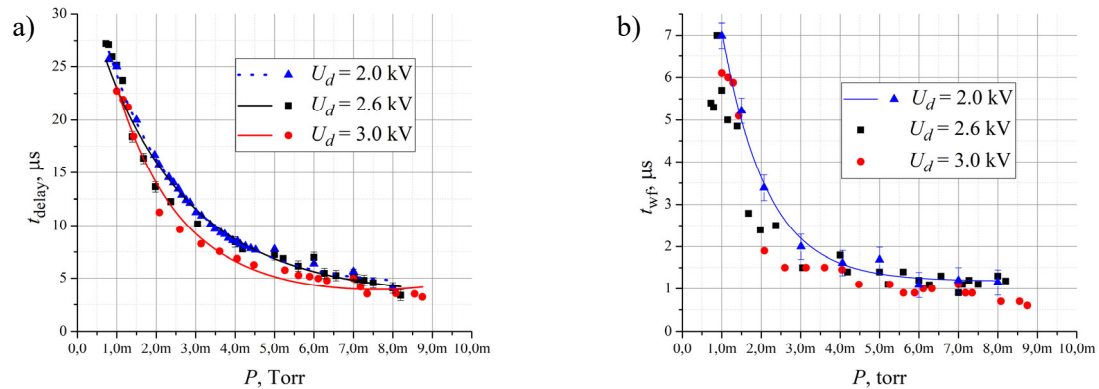


Figure 6. Dependence of the: a – delay time, b – front time in the pressure range 0.8–9 mTorr.

The influence of the magnetic field configuration and magnitude on discharge was also studied (see figure 7). It is shown that (for a given PIS geometry):

- Uniform magnetic field (B_z up to $\sim 90\text{ mT}$) compared to the non-uniform one increases the amplitude values of the discharge current pulse, with no significant improvement in the delay time. An increase in the discharge current above 1.5 mA (amplitude) does not lead to an increase in the extraction current of $400\ \mu\text{A}$;
- Uniform magnetic field (B_z up to $\sim 100\text{ mT}$) changes the discharge mode, resulting in the discharge current reaching 8mA, and the low extraction current was $300\ \mu\text{A}$. The discharge current reaches milliamper values already at pressure of 0.6 mTorr, although the level of the extraction current is at the level of $\sim 10\ \mu\text{A}$. The delay of 5–10 μs between the beginning of the discharge current pulse and the extraction current is observed;
- Inhomogeneous magnetic field with linearly decreasing value (from cathode to anticathode) improves the temporal parameters of the current outbreak, reduces the discharge current and improves recovery rates. At magnetic fields of 80–90 mT in the range of 4–7 mTorr the form of extraction current flash has a rectangular shape, and at increased pressure the time of a current delay falls from 10 to 5 μs , the time of a leading edge falls from 2 to 1 μs .

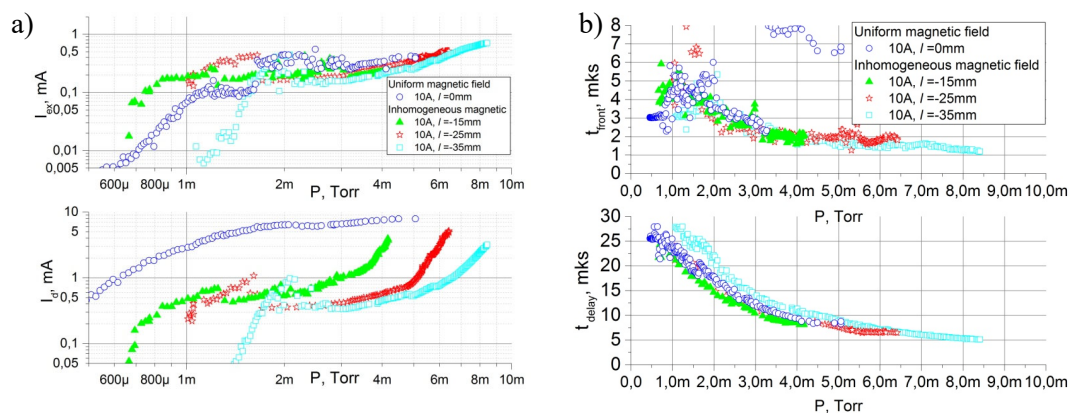


Figure 7. Comparison of the dependencies of the: a) discharge current I_d and extraction current I_{ex} ; b) delay time and the dependence of the front time on the pressure under impulse voltage ($U_a = 2\text{ kV}$, $f = 10\text{ kHz}$, $t_{\text{pulse}} = 30\ \mu\text{s}$) at various displacements of the solenoid relative to the center of the discharge cell, same current through the solenoid coil.

3. Conclusion

The discharge and extraction currents dependences on the pressure at constant and pulsed supply of PIS were determined. It was demonstrated the various (stable and unstable) regimes of the discharge depending on the power modes and their ranges of pressures. The amplitude-time characteristics and current-voltage characteristics were measured for different values and configurations (homogeneous and inhomogeneous) of the magnetic field in the discharge volume at fixed pressure. The features of the current oscillograph charts in the transition pressure range of 0.5–2 mTorr are determined.

References

- [1] Brown I G 1998 *The Physics and Technology of ion source* (New York, Chichester, Brisbane, Toronto, Singapore: A Wiley-Interscience Publication John Wiley&Sons)
- [2] Valkovic V 2016 *14 MeV Neutrons. Physics and Applications* (Boca Raton, London, New York: CRC Press Taylor&Francis Group)
- [3] Schuurman W 1967 *Physica* **36** 136
- [4] Hooper E B 1969 *Advances in Electronics and Electron Physics* (New York: Academic Press) **27** 295
- [5] Smirnitckaya G V and Nguyen-Khin-Tee Y 1969 *Herald of Moscow State University* **1** 3 (in Russian)
- [6] Reikhrudel E M, Smirnitckaya G V and Egiazarian G A 1973 *Soviet Phys.-Tech Phys.* XLIII **1** 130 (in Russian)
- [7] Kreindel Yu E 1977 *Plasma electron sources* (Moscow: Atomizdat) p 144 (in Russian)
- [8] Reikhrudel E M, Smirnitckaya G V and Nguyen-Khin-Tee Y 1969 *Soviet Phys.-Tech Phys.* XXXIX **6** 1052 (in Russian)
- [9] Sy A, Ji Q, Persaud A, Waldmann O and Schenkel T 2012 *Rev. Sci. Instrum.* **83** 1
- [10] Yan F, Jin D, Chen L and Xiao K 2018 *Nucl. Instrum. Method. Phys. Res. A* **906** 110
- [11] Das B K *et al* 2012 *Nucl. Instrum. Method. Phys. Res. A* **669** 19
- [12] Liu W *et al* 2014 *Nucl. Instrum. Method. Phys. Res. A* **768** 120
- [13] Li G, Zhang Z, Chi Q and Liu L 2012 *Nucl. Instrum. Method. Phys. Res. B* **290** 64
- [14] Mamedov N, Schitov N and Kanshin I 2016 *Instruments Experimental Techniques* **59** (6) 868
- [15] Rovey J L, Ruzic B P and Houlahan T J 2007 *Rev. Sci. Instrum.* **78** 106101
- [16] Liberman A D and Chen F K 1995 *Proc. SPIE* **2339** 188
- [17] Mamedov N, Schitov N *et al* 2018 *Technical Physics* **63** (8) 1129